IEEE Access
Multidisciplinary | Rapid Review | Open Access Journal

Received May 20, 2020, accepted June 6, 2020, date of publication June 10, 2020, date of current version June 24, 2020.

Digital Object Identifier 10.1109/ACCESS.2020.3001358

Adaptive Sensor Scheduling and Resource Allocation in Netted Collocated MIMO Radar System for Multi-Target Tracking

ZHENGJIE LI[1], JUNWEI XIE[1], HAOWEI ZHANG[1], HOUHONG XIANG[2], AND ZHAOJIAN ZHANG[3]

[1]Air and Missile Defense College, Air Force Engineering University, Xi'an 710051, China
[2]National Laboratory of Radar Signal Processing, Xidian University, Xi'an 710051, China
[3]Air Force Early Warning Academy of the PLA, Wuhan 410039, China

Corresponding author: Zhengjie Li (afeu_lzj@163.com)

This work was supported by the National Natural Science Foundation of China under Grant 61503408.

ABSTRACT In this paper, an effective solution for adaptive sensor scheduling integrated with power and bandwidth allocation is developed for centralized multiple target tracking (MTT) in the netted collocated multiple-input multiple-output (C-MIMO) radar system. By incorporating a modified particle filter, the predicted posterior Cramér-Rao lower bound (PCRLB) is calculated. Aiming at improving the sum of target tracking accuracy of location, the predicted PCRLBs for the location of multiple targets is derived as the optimization metric. Owing to the dynamic sensor scheduling is NP-hard, a convex relaxation technique is adopted for the sensor scheduling. Taking account of the problem of power and bandwidth allocation is non-convex, a joint convex relaxation technique and cycle minimizer algorithm is adopted to convert the non-convex optimization problem into a series of convex problems. After the results of resource allocation are fed back to each node, an adaptive closed-loop system is established. Numerical results demonstrate that the location tracking accuracy can be improved efficiently by the proposed algorithm.

INDEX TERMS Collocated MIMO radar, PCRLB, netted radar system, sensor scheduling, resource allocation.

I. INTRODUCTION

A. BACKGROUND AND MOTIVATION

The multistatic radar network has become a vigorous research field recently, given its great spatial diversity over the monostatic radar system [1]–[7]. For the collocated multiple-input multiple-output (C-MIMO) radar network system [3], [4], each C-MIMO radar can execute multiple radar tasks independently by launching multiple beams simultaneously in the simultaneous multibeam (SM) working mode [8]. Due to its high degree of freedom in waveform design, the C-MIMO radar is suitable and efficient in performing multiple target tracking (MTT) tasks [9]–[12]. Hence, the C-MIMO radar network can be effectively incorporated in MTT applications. However, the finite resources shall be efficiently managed so as to take full advantages of the spatial diversity and the waveform diversity of the C-MIMO radar network.

The associate editor coordinating the review of this manuscript and approving it for publication was Arun Prakash.

The monostatic C-MIMO radar system for MTT has been well studied in [9]–[13]. In practice, when a C-MIMO radar tracks multiple targets in the SM working mode, the target tracking accuracy of location is relevant with some limited system resources [10]–[12]: (i) *the maximum number of generated beams simultaneously*; (ii) *the total transmitting power from all beams*; (iii) *the total transmitting bandwidth from all beams.* In this case, for a monostatic C-MIMO radar system, how to manage these limited resources to maximize radar ability for MTT is of great importance. So far, the research on the resource allocation for MTT in the monostatic C-MIMO radar system is not sufficient. Reference [9] proposes a power allocation method for MTT in the monostatic C-MIMO radar system by using the SM working mode. Reference [10] develops a joint beam and power allocation scheme to further improve the C-MIMO radar's resource utilization. Reference [11] proposes a space-time allocation scheme in C-MIMO radar to further improve the freedom of transmit beam allocation. To improve the target tracking ability

of velocity, [12] discusses the joint power and time width allocation problem. In addition to the transmitting resource allocation, the antenna selection problem in the C-MIMO radar system for MTT has been studied in [13].

Regarding the netted C-MIMO system, the relevant researches of the resource allocation for MTT in the SM working mode are limited, and only appear in [3], [4] and [14]. Yan *et al*. [3] studied the resource management problem for MTT in the C-MIMO radar network system with the SM working mode initially, and proposed a joint beam and power allocation scheme under the ideal detection conditions. Based on [3], Lu *et al.* [4] further developed a joint scheduling and power allocation (JSPA) scheme with adjustable number of targets. Yi *et al.* [14] focused on the joint beam and power allocation problem for MTT in the netted C-MIMO radar system, and implemented a distributed fusion architecture based on the covariance intersection fusion to reduce the communication requirements among the C-MIMO radars.

In general, the existing researches on the resource allocation in the netted C-MIMO radar system mainly focus on the resources of beam and transmit power to improve the target tracking accuracy of location, but the bandwidth allocation is seldom covered until. However, for the MIMO radar system, one of the ways to achieve beam orthogonalization is to allocate multiple beams discrete bandwidth. Compared with other orthogonal beamforming techniques, this scheme can achieve waveform diversity by simple filtering mechanism. Moreover, each transmitter can be flexibly adjusted without affecting the orthogonality. In addition, Garcia *et al.* [15] proved that the bandwidth allocation can further improve the accuracy of target locating. Zhang *et al.* [16] studied a joint power and bandwidth allocation scheme for MTT in distributed MIMO radar, and bandwidth allocation was proven to improve the target tracking accuracy well. To the best of our knowledge, few studies focusing on the problem of bandwidth allocation in the C-MIMO radar network system with the SM working mode have been produced. As the bandwidth resource is vital in the target tracking problem, the bandwidth allocation must be taken into account.

B. MAIN CONTRIBUTION

In this paper, we intend to address the problem of the sensor scheduling integrated with power and bandwidth allocation for MTT in the netted C-MIMO radar system. Each C-MIMO radar in the network system works in the SM mode. In addition, the whole network system is operated in the centralized mode, where each node sends raw data to a common fusion center and this center allocates resources and conducts sensor scheduling. In practice, this fusion center can be easily established via wireless or cable communications and software supports [16].

The major contributions are given as follows:

(1) *An adaptive cognition tracking system for sensor scheduling integrated with power and bandwidth allocation is established*. We adopt a modified particle filter (shown in section III-A) to tackle the nonlinear filtering problem and acquire an accurate target state estimation. Due to its predictive ability, the posterior Cramér-Rao lower bound (PCRLB) is commonly used as an optimal criterion to guide the resource allocation [9]–[14], and [16]–[18]. Firstly, by using the target state estimation fusion information, the PCRLB at the next time is predicted. Secondly, the objective function related to transmit beam assignment integrated with power and bandwidth allocation is established by using the predicted PCRLB. Finally, the results of sensor scheduling and resource allocation are calculated by the fusion center and fed back to each C-MIMO radar to guide the task assignment for the next time. As such, a closed-loop feedback system is established, which can guide the adaptive allocation of system resources.

(2) *By introducing the convex relaxation technique and the cycle minimizer, the complex non-convex optimization problem is converted into a serious of easy-solving convex optimal problem.* Technically, the sensor scheduling problem is a 0-1 inter programming [5]–[7] and is NP-hard [19]. It can be solved via the exhaustive search [20], but the relevant computational burden will be huge for a large-scale C-MIMO network system. To meet the real-time demand, we adopt the convex relaxation of the node selection [21], so that the 0-1 inter programming problem can be converted into a convex optimization problem. For a given solution of sensor scheduling, the rest of resource allocation problem has become the non-convex optimization problem. After introducing the convex relaxation technique, the non-convex optimization problem can be converted into the convex optimization problem. In addition, a cycle minimizer solution could be leveraged to obtain the optimal solution of power and bandwidth allocation.

(3) *We build a bandwidth allocation scheme in the netted C-MIMO radar system for MTT with the SM working mode.* [15] proved that the joint power and bandwidth allocation can further improve the positioning accuracy of static target. In [16], a bandwidth allocation scheme is constructed in the distributed MIMO radar system for MTT, which shows a good performance in improving the target tracking accuracy. However, few studies have focused on the bandwidth allocation in C-MIMO radar. The simulation results demonstrate that bandwidth optimal allocation could outperform the bandwidth average allocation.

The remaining sessions of this paper are as follows. Section II describes the system model. Section III introduces the modified particle filter and then establishes the optimization model by deriving and integrating the location PCRLB of each C-MIMO radar. The solution of formulated sensor scheduling and resource allocation problem is proposed in section IV. Simulation results and analysis are described in section V. Section VII concludes this paper.

II. SYSTEM MODEL

Assume that a netted radar system is consist of totally $N \geq 3$ widely distributed C-MIMO radars located in 2-D space.

The radar system undertakes the target tracking role in the region of interest (ROI). The location of radar n is denoted as (x_n, y_n), where $n = 1, 2, \ldots, N$. Additionally, there are $Q \geq 3$ point-like targets moving in the ROI. For simplicity, we assume that the number of targets Q in the ROI is a constant and is known as prior information. For future use, we introduce a set of binary variables:

$$e_{n,q,k} = \begin{cases} 1, & \text{if target } q \text{ is tracked by radar } n \\ 0, & \text{otherwise} \end{cases} \tag{1}$$

where $q = 1, 2, \ldots, Q$, and $n = 1, 2, \ldots, N$. Therefore, the system model of sensor scheduling in the netted C-MIMO radar system can be intuitively depicted as Fig. 1.

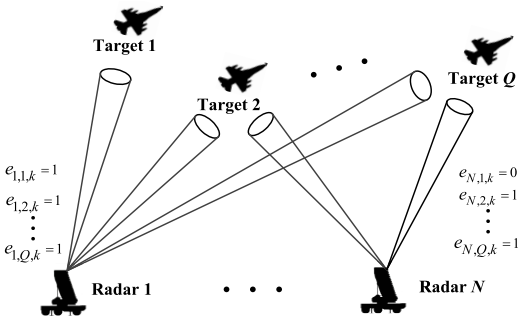

FIGURE 1. Work-flow of sensor scheduling in the netted C-MIMO radar system.

A. SIGNAL MODEL

To track these targets, each radar in the system adopts a SM working mode, where multiple orthogonal transmit beams are simultaneously generated and used to track different targets. The transmit signal from the nth radar to target q is normalized and orthogonal such that [16]

$$\int_{-\infty}^{+\infty} \left|s_{n,q}(t)\right|^2 \mathrm{d}t = 1, \quad q = 1, 2, \ldots, Q \tag{2}$$

$$\int_{-\infty}^{+\infty} s_{n,q}(t)\, s_{n,q'}^{H}(t-\tau)\mathrm{d}t = \begin{cases} 0, & q \neq q' \\ 1, & q = q' \end{cases} \tag{3}$$

In addition, consider that all transmit signals are narrowband with effective bandwidth [22]:

$$\beta_{n,k}^2 = \left(\int f^2 \left|S_{n,q}(f)\right|^2 \mathrm{d}f\right) \Big/ \left(\int \left|S_{n,q}(f)\right|^2 \mathrm{d}f\right) \tag{4}$$

and effective time duration:

$$T_{n,k}^2 = \left(\int t^2 \left|s_{n,q}(t)\right|^2 \mathrm{d}t\right) \Big/ \left(\int \left|s_{n,q}(t)\right|^2 \mathrm{d}t\right) \tag{5}$$

Therefore, the received signal from the qth target to radar n at the kth sample interval is

$$r_{n,q,k}(t) = a_{n,q,k} h_{n,q,k} s_{n,q}\left(t - \tau_{n,q,k}\right) \mathrm{e}^{\mathrm{j}2\pi f_{n,q,k} t} + n_{n,q,k}(t) \tag{6}$$

where $a_{n,q,k}$ represents the attenuation in the signal strength due to path loss effects, which satisfies that

$$a_{n,q,k} \propto \sqrt{P_{n,q,k}} \Big/ \left(R_{n,q,k}\right)^2 \tag{7}$$

where $P_{n,q,k}$ is the transmit power from radar n to target q, and $R_{n,q,k}$ is the distance between radar n and target q. The term $h_{n,q,k}$ represents the target reflectivity, which is modeled as a complex known variable. $\tau_{n,q,k}$ and $f_{n,q,k}$ denote the time delay and the Doppler frequency respectively. $n_{n,q,k}(t)$ represents a zero-mean, complex Guassian noise, which complies with $n_{n,q,k}(t) \sim \mathrm{N}(0, \sigma_{n,q}^2)$.

B. TARGET MOTION MODEL

Assume that the target motion model can be prescribed by a constant velocity (CV) model [23]:

$$\mathbf{x}_{q,k} = \mathbf{F}_q \mathbf{x}_{q,k-1} + \mathbf{w}_{q,k-1} \tag{8}$$

where $\mathbf{x}_{q,k} = [x_{q,k}, \dot{x}_{q,k}, y_{q,k}, \dot{y}_{q,k}]^{\mathrm{T}}$ is the state of target q at the kth sample interval. $\mathbf{F}_q$ denotes the state transition matrix in the CV model, and $\mathbf{w}_{q,k-1}$ is an uncorrelated process noise sequence which complies with $\mathbf{w}_{q,k-1} \sim \mathrm{N}(\mathbf{0}, \mathbf{Q}_{q,k-1})$. The math expression of $\mathbf{F}_q$ is given by [10]:

$$\mathbf{F}_q = \begin{bmatrix} 1 & T_0 \\ 0 & 1 \end{bmatrix} \otimes \mathbf{I}_2 \tag{9}$$

And $\mathbf{Q}_q$ can be calculated as:

$$\begin{aligned} \mathbf{Q}_{q,k-1} &= \mathbb{E}\left[\mathbf{w}_k^q \left(\mathbf{w}_k^q\right)^T\right] \\ &= \left(\int_0^{T_0} g_{q,k-1} \begin{bmatrix} T_0 - t \\ 1 \end{bmatrix} \begin{bmatrix} T_0 - t & 1 \end{bmatrix} \mathrm{d}t\right) \otimes \mathbf{I}_2 \\ &= g_{q,k-1} \begin{bmatrix} T_0^3/3 & T_0^2/2 \\ T_0^2/2 & T_0 \end{bmatrix} \otimes \mathbf{I}_2 \end{aligned} \tag{10}$$

where $\mathbb{E}$ denotes the mathematical expectation productor, and $g_{q,k-1}$ is the level of process noise intensity. T_0 is the sample time interval, and $\mathbf{I_2}$ represents a second-order identity matrix.

C. MEASUREMENT MODEL

Technically, there is a lot of target information in the radar receiving signal, which can be extracted by using the suitable signal processing methods [16]. In this paper, we focus on the range, Doppler frequency, and bearing angle. Therefore, with the combination of the binary variable $e_{n,q,k}$, the nth radar's measurement equation to the qth target at tracking interval k is defined as:

$$\mathbf{z}_{n,q,k} = \begin{cases} h_n\left(\mathbf{x}_{q,k}\right) + \mathbf{u}_{n,q,k} & \text{if } e_{n,q,k} = 1 \\ \mathbf{0} & \text{if } e_{n,q,k} = 0 \end{cases} \tag{11}$$

where $h_n(\cdot) = [h_R^n(\cdot), h_{\dot{r}}^n(\cdot), h_\theta^n(\cdot)]^{\mathrm{T}}$ represents the nonlinear measurement matrix. After substituting the target state $\mathbf{x}_{q,k}$

into $h_n(\cdot)$, the corresponding elements of the matrix are calculated as [3]:

$$\begin{cases} R_{n,q,k} = h_R^n\left(\mathbf{x}_{q,k}\right) = \sqrt{\left(x_{q,k}-x_n\right)^2+\left(y_{q,k}-y_n\right)^2} \\ f_{n,q,k} = h_{fd}^n\left(\mathbf{x}_{q,k}\right) = -\dfrac{2}{\lambda_n}\left(\dot{x}_{q,k}+\dot{y}_{q,k}\right) \\ \qquad\qquad \times \begin{pmatrix} x_{q,k}-x_n \\ y_{q,k}-y_n \end{pmatrix} \Big/ R_{n,q,k} \\ \theta_{n,q,k} = h_\theta^n\left(\mathbf{x}_{q,k}\right) = \arctan\left[\left(y_{q,k}-y_n\right)/\left(x_{q,k}-x_n\right)\right] \end{cases} \tag{12}$$

where λ_n is the carrier wavelength of the nth radar. In (11), $\mathbf{u}_{n,q,k}$ denotes the zero-mean Gaussian noise, who complies with $\mathbf{u}_{n,q,k}\sim\mathrm{N}(\mathbf{0},\mathbf{R}_{n,q,k})$. Suppose that the signal noise ratio (SNR) is high, thus we can define $\mathbf{R}_{n,q,k}$ as the CRLB matrix of the nth target's measurement error [24]:

$$\mathbf{R}_{n,q,k} = \mathrm{diag}\left(\sigma^2_{R_{n,q,k}}, \sigma^2_{f_{n,q,k}}, \sigma^2_{\theta_{n,q,k}}\right) \tag{13}$$

where $\sigma^2_{R_{n,q,k}}$, $\sigma^2_{f_{n,q,k}}$, and $\sigma^2_{\theta_{n,q,k}}$ are the CRLBs of the estimation errors of corresponding parameters [12]

$$\begin{cases} \sigma^2_{R_{n,q,k}} \propto \left(\alpha_{n,q,k}P_{n,q,k}\left|m_{n,q,k}\right|^2\beta^2_{n,q,k}\right)^{-1} \\ \sigma^2_{f_{n,q,k}} \propto \left(\alpha_{n,q,k}P_{n,q,k}\left|m_{n,q,k}\right|^2 T^2_{n,q,k}\right)^{-1} \\ \sigma^2_{\theta_{n,q,k}} \propto \left(\alpha_{n,q,k}P_{n,q,k}\left|m_{n,q,k}\right|^2 \Big/ B_{\mathrm{w}}\right)^{-1} \end{cases} \tag{14}$$

where $\beta_{n,q,k}$ and $T_{n,q,k}$ denote effective bandwidth and effective time width, respectively. $m_{n,q,k}$ denotes the target RCS. B_{W} is the null-to-null beam width of receive antenna [25].

III. RESOURCE OPTIMIZATION STRATEGY

A. MODIFIED PARTICLE FILTER

Due to the measurement model in Section II is nonlinear and is based on the multi-static system, the particle filter (PF) [26], which is known as a good tool in solving the nonlinear filtering problem, is adopted for state estimation. However, the standard PF directly obtains the importance function from the state transfer function, which may lead the problem of particle degradation [27]. The SCKF shares simple structure and high precision [28], which can provide an essential reference for selecting the important function in the PF. As such, the SCKF is applied to the framework of the PF so as to further improve its accuracy and stability. In this way, the modified PF can fully combine the advantages of the SCKF and the standard PF.

Suppose that the number of particles is B and the parameter to be estimated is the hybrid target state $\boldsymbol{\xi}_{q,k}$. Moreover, let $\boldsymbol{\xi}_{q,k|k-1}$ and $\boldsymbol{\xi}_{q,k|k}$ be the predicted state and the updated state vector of the qth target at interval k, with corresponding covariance matrices $\mathbf{Y}_{q,k|k-1}$ and $\mathbf{Y}_{q,k|k}$, respectively. With the combination of Section II, the SCPF can be described as follows.

Step 1: Initialization. Let $k = 0$, suppose an initial PDF $p(\boldsymbol{\xi}_{q,k+1|k})$, $q = 1, 2, \ldots, Q$. Therefore, according to $p(\boldsymbol{\xi}_{q,k+1|k})$, the particles state $\boldsymbol{\xi}_{b,q,k+1|k}$ can be obtained, $b = 1, 2, \ldots, B$.

Step 2: Filtering update. By substituting $\boldsymbol{\xi}_{b,q,k+1|k}$ and the measurement information $\mathbf{z}_{q,k+1} = \{\mathbf{z}_{n,q,k+1}\}_{n=1}^N$ into the SCKF, the sample mean $\bar{\mathbf{x}}_{q,k+1|k}$ and the corresponding covariance $\bar{\mathbf{U}}_{q,k+1|k}$ can be calculated. All the calculations details can be found in [28]. Then, the updated particles state $\boldsymbol{\xi}_{b,q,k+1|k} \sim \mathrm{N}(\bar{\mathbf{x}}_{q,k+1|k}, \bar{\mathbf{U}}_{q,k+1|k})$ and then the corresponding importance sampling function $q(\boldsymbol{\xi}_{b,q,k+1|k}|\boldsymbol{\xi}_{b,q,k|k}, \mathbf{z}_{q,k+1})$ can be obtained.

Step 3: Weight calculation and normalization.

$$w_{b,q,k+1} = w_{b,q,k} \times \frac{p\left(\mathbf{z}_{q,k+1}\left|\boldsymbol{\xi}_{b,q,k+1|k}\right.\right) p\left(\boldsymbol{\xi}_{b,q,k+1|k}\left|\boldsymbol{\xi}_{b,q,k}\right.\right)}{q\left(\boldsymbol{\xi}_{b,q,k+1|k}\left|\boldsymbol{\xi}_{b,q,k|k}, \mathbf{z}_{q,k+1}\right.\right)} \tag{15}$$

$$\tilde{w}_{b,q,k+1} = w_{b,q,k+1} \Big/ \sum_{b=1}^{B} w_{b,q,k+1} \tag{16}$$

Step 4: Resampling. According to the important weight $\tilde{w}_{b,q,k+1}$, $\boldsymbol{\xi}_{b,q,k+1|k}$ is resampled as $\bar{\boldsymbol{\xi}}_{b,q,k+1|k}$, $b = 1, 2, \ldots, B$. In addition, let $w_{b,q,k+1} = 1/N$, $b = 1, 2, \ldots, B$.

Step 5: State update.

$$\boldsymbol{\xi}_{q,k+1|k+1} = \sum_{b=1}^{B} w_{b,q,k+1}\bar{\boldsymbol{\xi}}_{b,q,k+1|k} \tag{17}$$

$$\mathbf{Y}_{q,k+1|k+1} = \sum_{b=1}^{B} w_{b,q,k+1}\left(\bar{\boldsymbol{\xi}}_{b,q,k+1|k} - \boldsymbol{\xi}_{q,k+1|k+1}\right) \times \left(\bar{\boldsymbol{\xi}}_{b,q,k+1|k} - \boldsymbol{\xi}_{q,k+1|k+1}\right)^{\mathrm{T}} \tag{18}$$

Step 6: Recursion. Let $k = k + 1$, propagate $\boldsymbol{\xi}_{b,q,k+1|k}$ according to $\boldsymbol{\xi}_{b,q,k+1|k} = F_q, \boldsymbol{\xi}_{b,q,k|k} + \mathfrak{R}_{b,q,k|k}$ ($\mathfrak{R}_{b,q,k|k} \sim \mathrm{N}(\mathbf{0},\mathbf{Y}_{q,k|k})$), and return to *step 2*.

B. PERFORMANCE METRIC

Since the PCRLB provides a lower bound for the target tracking error and shares predictive ability [29], we adopt the PCRLB as the performance metric in the resource allocation problem. Thus, the PCRLB inequality can be written as [30]:

$$\mathbb{E}_{\boldsymbol{\xi}_{q,k},\mathbf{z}_{q,k}}\left[\left(\hat{\boldsymbol{\xi}}_{q,k}\left(\mathbf{z}_{q,k}\right) - \boldsymbol{\xi}_{q,k}\right)\left(\hat{\boldsymbol{\xi}}_{q,k}\left(\mathbf{z}_{q,k}\right) - \boldsymbol{\xi}_{q,k}\right)^{\mathrm{T}}\right] \geq \mathbf{J}^{-1}\left(\boldsymbol{\xi}_{q,k}\right) \tag{19}$$

where $\hat{\boldsymbol{\xi}}_{q,k}(\mathbf{z}_{q,k})$ is the unbiased estimation of $\boldsymbol{\xi}_{q,k}$, and is obtained by the SCPF algorithm. $\mathbf{J}(\boldsymbol{\xi}_{q,k})$ is the Bayesian Fisher information matrix (BFIM), and also the inverse of the PCRLB. Previously, the PCRLB for the sensor scheduling problem in the netted C-MIMO radar system has already been derived in [3]

$$\mathbf{J}\left(\boldsymbol{\xi}_{q,k}\right) = \left[\mathbf{Q}_{q,k-1} + \mathbf{F}_q\mathbf{J}^{-1}\left(\boldsymbol{\xi}_{q,k-1}\right)\mathbf{F}_q^{\mathrm{T}}\right]^{-1} + \sum_{n=1}^{N}\mathbb{E}_{\boldsymbol{\xi}_{q,k}}\left[e_{n,q,k}\left(\mathbf{H}_{n,q,k}\right)^{\mathrm{T}}\left(\mathbf{R}_{n,q,k}\right)^{-1}\mathbf{H}_{n,q,k}\right] \tag{20}$$

where $\mathbf{H}_{n,q,k}$ is the Jacobian matrix related to $\boldsymbol{\xi}_{q,k}$ and satisfies that $\mathbf{H}_{n,q,k} = [\Delta_{\boldsymbol{\xi}_{q,k}} h_n(\boldsymbol{\xi}_{q,k})]^{\mathrm{T}}$. However, solving (20) by using the Monte Carlo technique [31] is time-consuming and not cost-effective. In practice, to satisfy the real-time demand, the following approximation is formed [16]

$$\mathbf{J}\left(\boldsymbol{\xi}_{q,k}\right) = \left[\mathbf{Q}_{q,k-1} + \mathbf{F}_q \mathbf{J}^{-1}\left(\boldsymbol{\xi}_{q,k-1}\right) \mathbf{F}_q^{\mathrm{T}}\right]^{-1} + \sum_{n=1}^{N} \left[e_{n,q,k} \left(\hat{\mathbf{H}}_{n,q,k}\right)^{\mathrm{T}} \left(\hat{\mathbf{R}}_{n,q,k}\right)^{-1} \hat{\mathbf{H}}_{n,q,k} \right] \quad (21)$$

where $\hat{\mathbf{H}}_{n,q,k}$ and $\hat{\mathbf{R}}_{n,q,k}$ are the Jacobian and measurement covariance matrices evaluated around $\boldsymbol{\xi}_{q,k|k-1}$ which denotes the one-step prediction vector of $\boldsymbol{\xi}_{q,k-1}$ in the zero process noise condition. Apparently, the results of the sensor selection will contribute to $\mathbf{J}(\boldsymbol{\xi}_{q,k})$ in (21). In addition, from (7) and (13)-(14), it is obvious that the allocation results of $P_{n,q,k}$ and $\beta_{n,q,k}$ can effect $\mathbf{R}_{n,q,k}$ and then effect $\mathbf{J}(\boldsymbol{\xi}_{q,k})$. However, in practice, when effective bandwidth is adjusted, the corresponding time width will change consequently, leading to an intractable case. To avoid the heterogeneous phenomenon between position and velocity, we extract the position PCRLB to replace the whole PCRLB. In the following parts, all the mentioned PCRLBs are the location PCRLBs.

C. OBJECTIVE FUNCTION

To describe the problem of power and bandwidth allocation in the sensor scheduling process, we further define the power allocation variable $P_{n,q,k}$ and bandwidth allocation variable $\beta_{n,q,k}$. As such, combining these variables with the results of the beam selection, three vectors are established:

$$\begin{cases} \mathbf{e}_k = \left[\mathbf{e}_{1,k}, \mathbf{e}_{2,k}, \ldots, \mathbf{e}_{Q,k}\right]^{\mathrm{T}} \\ \mathbf{P}_k = \left[\mathbf{P}_{1,k}, \mathbf{P}_{2,k}, \ldots, \mathbf{P}_{Q,k}\right]^{\mathrm{T}} \\ \boldsymbol{\beta}_k = \left[\boldsymbol{\beta}_{1,k}, \boldsymbol{\beta}_{2,k}, \ldots, \boldsymbol{\beta}_{Q,k}\right]^{\mathrm{T}} \end{cases} \quad (22)$$

where $\mathbf{e}_{q,k} = [e_{1,q,k}, e_{2,q,k}, \ldots, e_{N,q,k}]^{\mathrm{T}}$, $\mathbf{P}_{q,k} = [P_{1,q,k}, P_{2,q,k}, \ldots, P_{N,q,k}]^{\mathrm{T}}$, and $\boldsymbol{\beta}_{q,k} = [\beta_{1,q,k}, \beta_{2,q,k}, \ldots, \beta_{N,q,k}]^{\mathrm{T}}$. $P_{n,q,k}$ and $\beta_{n,q,k}$ can refer to (7), (13) and (14). Therefore, combining the above with section III-B, the predictive PCRLB of the qth target can be defined as:

$$\mathbb{C}_{PCRLB}\left(\mathbf{e}_{q,k}, \mathbf{P}_{q,k}, \boldsymbol{\beta}_{q,k}\right)\big|_{\boldsymbol{\xi}_{q,k}} = \mathbf{J}^{-1}\left(\boldsymbol{\xi}_{q,k}, \mathbf{e}_{q,k}, \mathbf{P}_{q,k}, \mathbf{T}_{q,k}\right) \quad (23)$$

In this paper, we focus on the sum of the target tracking accuracy. Therefore, the objective function is set as:

$$\min \mathbb{F}\left(\mathbf{e}_k, \mathbf{P}_k, \boldsymbol{\beta}_k\right) = \min \left\{ \sum_{q=1}^{Q} \sqrt{\mathrm{tr}\left[\mathbb{C}_{PCRLB}\left(\mathbf{e}_{q,k}, \mathbf{P}_{q,k}, \boldsymbol{\beta}_{q,k}\right)\big|_{\boldsymbol{\xi}_{q,k}} \right]} \right\} \quad (24)$$

IV. SENSOR SCHEDULING INTEGRATED WITH POWER AND BANDWIDTH ALLOCATION

A. OPTIMIZATION MODEL

Practically, a netted C-MIMO radar system does not always appoints all the nodes to track a known target, given the limitation on transmission rate, communication bandwidth, and computational complexity [5]. Additionally, restricted by the degrees of freedom, the maximum number of orthogonal beams simultaneously generated by a C-MIMO radar is a constant. Therefore, we assume that only $L \geq 2$ nodes can be selected to track one target in the ROI at each sample interval. Besides, for simplicity, we suppose that each radar can generate at most $M \geq 2$ orthogonal beams simultaneously.

Additionally, the total power $P_{n,\mathrm{total}}$ and total bandwidth $\beta_{n,\mathrm{total}}$ of the nth radar are limited. When the selection variable $e_{n,q,k} = 1$, the corresponding transmit power $P_{n,\mathrm{q},k}$ and effective bandwidth $\beta_{n,q,k}$ should be considered as the variables to be assigned. Based on the above analysis and assumptions, the optimization model is formulated as:

$$\begin{aligned} &\min \ \mathbb{F}\left(\mathbf{e}_k, \mathbf{P}_k, \boldsymbol{\beta}_k\right) \\ &\text{s.t.} \ \sum_{q=1}^{Q} e_{n,q,k} P_{n,q,k} = P_{n,\mathrm{total}}, \quad \sum_{q=1}^{Q} e_{n,q,k} \beta_{n,q,k} = \beta_{n,\mathrm{total}} \\ &\quad \sum_{n=1}^{N} e_{n,q,k} = L, \quad \sum_{q=1}^{Q} e_{n,q,k} \leq M, e_{n,q,k} \in \{0, 1\} \\ &\quad \bar{P}_{n,\min} \leq P_{n,q,k} \leq \bar{P}_{n,\max}, \quad \bar{\beta}_{n,\min} \leq \beta_{n,q,k} \leq \bar{\beta}_{n,\max} \\ &\quad \forall n = 1, 2, \ldots, N, \quad \forall q = 1, 2, \ldots, Q \end{aligned} \quad (25)$$

where the first constraint denotes the limitation of the total power and bandwidth budget of each radar, while the second one limits the number of the radars to be selected and the maximum number of the transmit beams in each radar. In addition, the third condition denotes the limitation of the transmit power and the effective bandwidth, where $\bar{P}_{n,\min}$ and $\bar{P}_{n,\max}$ denote the lower and upper bounds of the transmit power of radar n, while $\bar{\beta}_{n,\min}$ and $\bar{\beta}_{n,\max}$ represent the lower and upper bounds of the effective bandwidth.

Accordingly, the sensor scheduling integrated with power and bandwidth allocation scheme is established. After the solutions of (25) are sent back to each C-MIMO radar, a closed-loop tracking system can be formed which is shown in Fig. 2.

B. SOLUTION STRATEGY

From mathematics' perspective, (25) demonstrates that beam selection integrated with power and bandwidth allocation for multiple target tracking in the netted C-MIMO radar system is an optimization problem. However, due to the existence of the binary and the continuous variables, the optimization problem in (25) is non-convex [3]–[5]. To solve the non-convex optimization problem, we propose a three-step solution technique.

Step 1: Sensor selection with uniformly allocated power and bandwidth. In this case, assume that the transmit power and effective bandwidth of each beam from each radar are uniformly allocated and thus, the optimization formulation

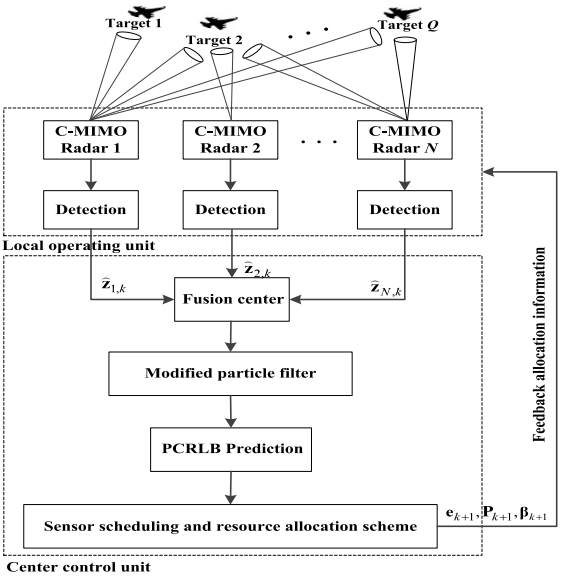

FIGURE 2. Framework of recognition tracking system.

can be rewritten as:

$$\begin{aligned}&\min\ \mathbb{F}(\mathbf{e}_k)\\&\text{s.t.}\ \sum_{n=1}^{N} e_{n,q,k}=L,\quad \sum_{q=1}^{Q} e_{n,q,k}\le M,\quad e_{n,q,k}\in\{0,1\}\\&\quad \forall n=1,2,\ldots,N,\quad \forall q=1,2,\ldots,Q\end{aligned}\tag{26}$$

Due to the set of binary variables $\mathbf{e}_k$, (26) is known as a NP-hard problem in [5], [6] and [16]. To tackle this problem, we introduce a convex relaxation technique [18], by replacing the binary constraint $e_{n,q,k}\in\{0,1\}$ with convex constraints $e_{n,q,k}\in[0,1]$, and then (26) can be converted to the convex optimization problem [7]. In addition, the convex problem can be further converted to the SDP problem [32]. Therefore, (26) can be formulated as:

$$\begin{aligned}&\min\ \sum_{q=1}^{Q}\sqrt{\mathrm{tr}\left[\mathbf{M}_{q,k}\right]}\\&\text{s.t.}\ \begin{bmatrix}\mathbb{M}_{q,k} & \mathbf{I}\\ \mathbf{I} & \mathbf{J}(\mathbf{e}_{q,k})\end{bmatrix}\ge 0\\&\quad \sum_{n=1}^{N} e_{n,q,k}=L,\quad \sum_{q=1}^{Q} e_{n,q,k}\le M,\quad 0\le e_{n,q,k}\le 1\\&\quad \forall n=1,2,\ldots,N,\quad \forall q=1,2,\ldots,Q\end{aligned}\tag{27}$$

where $\mathbf{M}_q$ is an auxiliary matrix, which satisfies that $\mathbf{M}_{q,k}\ge\mathbf{J}^{-1}(\mathbf{e}_{q,k})$. Thus, (28) can be easily solved by the modified Frank-Wolfe feasible direction method, which is shown in Table 1.

It should be note that the solution $\mathbf{e}_k$ for the relaxed problem (27) can be fractional. To obtain a suboptimal solution of the sensor selection problem, we shall find the L largest elements in $\{e_{n,q,k}\}_{n=1}^{N}$, and generate a corresponding suboptimal sensor selection result $\hat{\mathbf{e}}_k$.

TABLE 1. Modified Frank-Wolfe feasible direction method.

(1) Reformulation. The optimization model is normalized as :

$$\begin{aligned}&\min f(\mathbf{x})\\&\text{s.t.}\ \mathbf{Ax}\ge\mathbf{b}\\&\quad \mathbf{Ex}=\mathbf{e}\end{aligned}$$

Then, input an initial feasible point $\mathbf{x}^{(1)}$, set the allowable error $\xi>0$ and $k=1$.

(2) Solving the following linear programming model:

$$\begin{aligned}&\min \nabla f(\mathbf{x}^{(k)})^{\mathrm{T}}\mathbf{x}\\&\text{s.t.}\ \mathbf{Ax}\ge\mathbf{b}\\&\quad \mathbf{Ex}=\mathbf{e}\end{aligned}$$

Then, obtain the optimal solution $\mathbf{y}^{(k)}$.

(3) If $|\nabla f(\mathbf{x}^{(k)})^{\mathrm{T}}(\mathbf{y}^{(k)}-\mathbf{x}^{(k)})|\le\xi$, stops and outputs $\mathbf{x}^{(k)}$. Otherwise, go to (4).

(4) Solve

$$\begin{aligned}&\min f(\mathbf{x}^{(k)}+\lambda(\mathbf{y}^{(k)}-\mathbf{x}^{(k)}))\\&\text{s.t.}\quad 0\le\lambda\le\lambda_{\max}\end{aligned}$$

And obtain the optimal $\lambda^{(k)}$.

(5) Let $\mathbf{x}^{(k+1)}=\mathbf{x}^{(k)}+\lambda^{(k)}(\mathbf{y}^{(k)}-\mathbf{x}^{(k)})$, and set $k=k+1$, return to (2)

Step 2: Joint power and bandwidth allocation of individual radar. After the sensor selection solution $\hat{\mathbf{e}}_k$ is obtained, our optimization problem is to allocate the limited power and bandwidth resource of each radar to its own multiple beams. The optimization formulation is

$$\begin{aligned}&\min\ \mathbb{F}\left(\mathbf{P}_k,\boldsymbol{\beta}_k\right)\big|_{\hat{\mathbf{e}}_k}\\&\text{s.t.}\ \sum_{q=1}^{Q}\hat{e}_{n,q,k}P_{n,q,k}=P_{n,\text{total}},\quad \sum_{q=1}^{Q}\hat{e}_{n,q,k}\beta_{n,q,k}=\beta_{n,\text{total}}\\&\quad \bar{P}_{n,\min}\le P_{n,q,k}\le\bar{P}_{n,\max},\quad \bar{\beta}_{n,\min}\le\beta_{n,q,k}\le\bar{\beta}_{n,\max}\\&\quad \forall n=1,2,\ldots,N,\quad \forall q=1,2,\ldots,Q\end{aligned}\tag{28}$$

However, due to the effective bandwidth exists as the form of quadratic in (14), (28) is a non-convex problem. To tackle this problem, we set the bandwidth allocation as the uniformity firstly, then

Step 2.1: Solve the transient power allocation. On the condition of uniformly bandwidth allocation, (28) can be calculated as

$$\begin{aligned}&\min\mathbb{F}\left(\mathbf{P}_k|_{\hat{\mathbf{e}}_k}\right)\\&\text{s.t.}\ \sum_{q=1}^{Q}\hat{e}_{n,q,k}P_{n,q,k}=P_{n,\text{total}}\\&\quad \overline{P}_{n,\min}\le P_{n,q,k}\le\overline{P}_{n,\max}\\&\quad \forall n=1,2,\ldots,N,\quad \forall q=1,2,\ldots,Q\end{aligned}\tag{29}$$

As (29) is a convex optimization problem [4], [5], and thus (29) can be converted into SDP problem similar to (27).

Then, we have

$$\begin{aligned}
&\min \sum_{q=1}^{Q} \sqrt{\mathrm{tr}\left\{\mathbf{N}_{q,k}\right\}} \\
&\text{s.t.} \begin{bmatrix} \mathbf{N}_{q,k} & \mathbf{I} \\ \mathbf{I} & \mathbf{J}(\mathbf{P}_{q,k})\big|_{\hat{\boldsymbol{e}}_{q,k}} \end{bmatrix} \geq 0 \\
&\sum_{q=1}^{Q} \hat{e}_{n,q,k} P_{n,q,k} = P_{n,\text{total}}, \quad \overline{P}_{n,\min} \leq P_{n,q,k} \leq \overline{P}_{n,\max}, \\
&\forall n = 1, 2, \ldots, N, \quad \forall q = 1, 2, \ldots, Q
\end{aligned} \tag{30}$$

where $\mathbf{N}_{q,k}$ is an auxiliary matrix, which satisfies that $\mathbf{N}_{q,k} \geq \mathbf{J}^{-1}(\mathbf{P}_{q,k})\big|_{\hat{\mathbf{e}}_{q,k}}$. Similar to (27), (30) can be efficiently solved by the modified Frank-Wolfe feasible direction method, and then we can obtain the suboptimal power allocation $\hat{\mathbf{P}}_k$.

Step 2.2: Solve the transient bandwidth allocation. Set the power allocation as $\hat{\mathbf{P}}_k$, temporarily. Therefore, (28) can be reformulated as

$$\begin{aligned}
&\min \mathbb{F}\left(\boldsymbol{\beta}_k\big|_{\hat{\mathbf{e}}_k}\right) \\
&\text{s.t.} \sum_{q=1}^{Q} \hat{e}_{n,q,k} \beta_{n,q,k} = \beta_{n,\text{total}} \\
&\overline{\beta}_{n,\min} \leq \beta_{n,q,k} \leq \overline{\beta}_{n,\max} \\
&\forall n = 1, 2, \ldots, N, \quad \forall q = 1, 2, \ldots, Q
\end{aligned} \tag{31}$$

However, due to the quadratic form of $\beta_{n,q,k}$, (31) is non-convex problem which is difficult to solve. To deal with this problem, we utilize a convex relaxation technique by introducing a new vector: $\boldsymbol{\gamma}_k = [\boldsymbol{\gamma}_{1,k}, \boldsymbol{\gamma}_{2,k}, \ldots, \boldsymbol{\gamma}_{Q,k}]^{\mathrm{T}}$, where $\boldsymbol{\gamma}_{q,k} = [\gamma_{1,q,k}, \gamma_{2,q,k}, \ldots, \gamma_{N,q,k}]^{\mathrm{T}} = [|\beta_{1,q,k}|^2, |\beta_{2,q,k}|^2, \ldots, |\beta_{N,q,k}|^2]^{\mathrm{T}}$, $q = 1, 2, \ldots, Q$. Therefore, (31) can be converted into

$$\begin{aligned}
&\min \mathbb{F}\left(\boldsymbol{\gamma}_k\big|_{\hat{\mathbf{e}}_k}\right) \\
&\text{s.t.} \sum_{q=1}^{Q} \hat{e}_{n,q,k} \gamma_{n,q,k} \leq \lambda_1 \left(\beta_{n,\text{total}}\right)^2 \\
&\sum_{q=1}^{Q} \hat{e}_{n,q,k} \left(\gamma_{n,q,k}\right)^{1/2} \geq \lambda_2 \beta_{n,\text{total}} \\
&\left|\overline{\beta}_{n,\min}\right|^2 \leq \gamma_{n,q,k} \leq \left|\overline{\beta}_{n,\max}\right|^2 \\
&\forall n = 1, 2, \ldots, N, \quad \forall q = 1, 2, \ldots, Q
\end{aligned} \tag{32}$$

where λ_1 and λ_2 are both dynamic parameters, which can be adjusted according to the simulation results. Similar to (29), (32) is a convex optimization problem because of the first order variables $\gamma_{n,q,k}$, $n = 1, 2, \ldots N$, and $q = 1, 2, \ldots, Q$.

Similar to (27) and (30), the SDP form of (32) is

$$\begin{aligned}
&\min \sum_{q=1}^{Q} \sqrt{\mathrm{tr}\left\{\mathbf{S}_{q,k}\right\}} \\
&\text{s.t.} \begin{bmatrix} \mathbf{S}_{q,k} & \mathbf{I} \\ \mathbf{I} & \mathbf{J}(\boldsymbol{\gamma}_{q,k})\big|_{\hat{\boldsymbol{e}}_{q,k}} \end{bmatrix} \geq 0 \\
&\sum_{q=1}^{Q} \hat{e}_{n,q,k} \gamma_{n,q,k} \leq \lambda_1 \left(\beta_{n,\text{total}}\right)^2 \\
&\sum_{q=1}^{Q} \hat{e}_{n,q,k} \left(\gamma_{n,q,k}\right)^{1/2} \geq \lambda_2 \beta_{n,\text{total}} \\
&\left|\overline{\beta}_{n,\min}\right|^2 \leq \gamma_{n,q,k} \leq \left|\overline{\beta}_{n,\max}\right|^2 \\
&\forall n = 1, 2, \ldots, N, \quad \forall q = 1, 2, \ldots, Q
\end{aligned} \tag{33}$$

where $\mathbf{s}_{q,k}$ is an auxiliary matrix, which satisfies that $\mathbf{N}_{q,k} \geq \mathbf{J}^{-1}(\boldsymbol{\gamma}_{q,k})\big|_{\hat{\mathbf{e}}_{q,k}}$. Therefore, (33) can be solved by the modified Frank-Wolfe feasible direction method, and as a result of which, the transient bandwidth allocation $\hat{\boldsymbol{\beta}}_k$ can be obtained.

Step 2.3: Further improve the bandwidth allocation solution precision. To improve the precision of the transient bandwidth allocation solution $\hat{\boldsymbol{\beta}}_k$, we propose a local search algorithm shown in Table 2. Firstly, let $\hat{\boldsymbol{\beta}}_k = [\hat{\boldsymbol{\beta}}_{1,k}, \hat{\boldsymbol{\beta}}_{2,k}, \ldots, \hat{\boldsymbol{\beta}}_{N,k}]$, and $\hat{\boldsymbol{\beta}}_{n,k} = [\hat{\boldsymbol{\beta}}_{n,1,k}, \hat{\boldsymbol{\beta}}_{n,2,k}, \ldots, \hat{\boldsymbol{\beta}}_{n,Q,k}]$, n = 1, 2, ..., N. Secondly, set $\hat{\boldsymbol{\beta}}_k$ as the initial point for the local search algorithm. Thirdly, we reduce one of elements in $\hat{\boldsymbol{\beta}}_{n,k}$ by $\Delta\beta$, and add $\Delta\beta$ to any of other element, to generate a new vector $\hat{\boldsymbol{\beta}}_k^{+}$. Then, the bandwidth solution corresponding to the minimum value of the cost function is taken as the initial solution at the next iteration. Finally, the process stops until the deduction of the cost function in one iteration to another is satisfied the stopping condition ε.

TABLE 2. Local search algorithm for (32).

(1) Initialization: $\boldsymbol{\beta}_0 = \hat{\boldsymbol{\beta}}_k$ (solved by (32) and reordered by *step 2.3*), $\mathbf{P} = \hat{\mathbf{P}}_k$ (solved by (30)), iteration step $\Delta\beta$ and stop condition ε.

(2) Repeat $\boldsymbol{\beta}_l$ =argmax $\{\mathbb{F}(\mathbf{P}, \boldsymbol{\beta}_{l-1}^{+})\text{-}\mathbb{F}(\mathbf{P}, \boldsymbol{\beta}_{l-1})\}$
s.t. $\overline{\beta}_{n,\min} \leq \beta_{n,q,k} \leq \overline{\beta}_{n,\max}$
$\Delta\beta_l = \Delta\beta_{l-1}(\mathbf{1}_Q^{\mathrm{T}} \mathbf{1}_Q \boldsymbol{\beta}_{n,l} / \mathbf{1}_Q^{\mathrm{T}} \boldsymbol{\beta}_{n,l-1})$

(3) while $\mathbb{F}(\mathbf{P}, \boldsymbol{\beta}_{l-1})\text{-}\mathbb{F}(\mathbf{P}, \boldsymbol{\beta}_l) \geq \varepsilon$,
set $\boldsymbol{\beta}_{\text{MLE}} = \boldsymbol{\beta}_{l-1}$,
end

Step 3: Record and return. Record the current resource allocation results and the corresponding cost function values at each interval. Then, return to *step 1*, and stop when the

difference between the twice values of the cost function satisfies the end condition φ. When the loop ends, record the smaller values of the cost function as the final results, and separate the corresponding resource allocation results as the final optimal resource allocation results.

C. COMPUTATIONAL COMPLEXITY ANALYSIS

Technically, the computational complexity of the proposed solution strategy is mainly determined by the iterations of the SDP problem. Considering the structures of the optimization formulations (30) and (33) are similar, and thus the relevant computational complexity is the same [5]. Consequently, the proposed solution strategy has the worst-case computational complexity of $\mathrm{O}\left(Q\left(M+2\right)\right) \approx \mathrm{O}\left(QM\right)$. By contrast, the exhaustive search algorithm needs an exponential complexity of $\mathrm{O}\left(Q\sum_{m=1}^{M} C_N^L\right)$. As a result, compared with the exhaustive search algorithm, our proposed method can evidently reduce the computational complexity especially in a large-scale optimization problem. In addition, this observation can be verified in simulations.

V. SIMULATION RESULTS AND ANALYSIS

In this section, simulation results are presented to demonstrate the effectiveness of the method we proposed. A netted C-MIMO radar system with $N = 16$ spatially diverse C-MIMO radars is used to perform the analysis. For simplicity, we assume that each C-MIMO radar could perform in the same way. Also the total transmit power of the nth radar is set as $P_{n,\mathrm{total}} = 20\mathrm{kW}$, the total effective bandwidth of the nth radar is $\beta_{n,\mathrm{total}} = 2\mathrm{MHz}$, and the total effective time width of the nth radar is $T_{n,\mathrm{total}} = 1\mathrm{ms}$, and the carrier wavelength of the nth radar is set as $\lambda_n = 0.3\mathrm{m}$, $n = 1, 2, \ldots, N$. There are $Q = 3$ widely separated targets, and all the targets follow the CV model with the initial parameters of each target specified in Table 3. The joint configuration of the radar system and the targets is shown in Fig. 3. A sequence of 20 frames are used in each Monte Carlo trial with sample interval $T_s = 5\mathrm{s}$, while the number of Monte Carlo trial $N_{\mathrm{sim}} = 100$. The number of particles is set to $B = 200$. In addition, the lower and upper bounds of the transmit power are $\bar{P}_{n,\min} = 0$ and $\bar{P}_{n,\max} = 0.8P_{n,\mathrm{total}}$, while the corresponding effective bandwidth bounds are $\bar{\beta}_{n,\min} = 0$ and $\bar{\beta}_{n,\max} = 0.8\beta_{n,\mathrm{total}}$. For brevity, the maximum beam number of each radar is set as $M = 3$, and the maximum number of radars to be selected for each target is $L = 10$.

TABLE 3. The initial parameters of each target.

Target index	1	2	3
Position (km)	(65.89,54.75)	(62.06,44.75)	(73.95,25.54)
Velocity (m/s)	(-290,-200)	(-140,-250)	(-50,264)

Moreover, to illustrate the utilization of proposed method in improving the target tracking precision, the total location

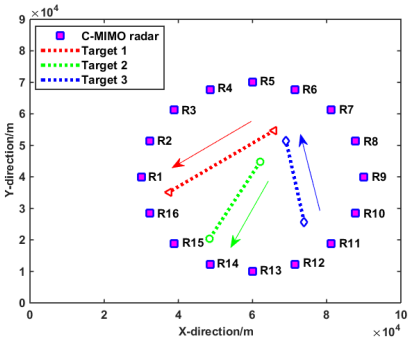

FIGURE 3. Netted radar system configuration and targets deployment.

root mean square error (RMSE) at interval k is proposed as

$$RMSE_k = \sum_{q=1}^{Q} \sqrt{\frac{1}{N_{\mathrm{sim}}} \sum_{j=1}^{N_{\mathrm{sim}}} \left((x_{q,k} - \widehat{x}_{q,k,j})^2 + (y_{q,k} - \widehat{y}_{q,k,j})^2 \right)} \tag{34}$$

where $(\widehat{x}_{q,k,j}, \widehat{y}_{q,k,j})$ denotes the location estimation of the qth target at the jth trial. In addition, to further reveal the effects of the distance of target to radar and the target RCS on the resource allocation results, two RCS models are considered ($\mathbf{M}_1$, $\mathbf{M}_2$). In the first RCS model $\mathbf{M}_1$, we mainly consider the distance effects and thus we set $m_{n,q,k} = 1$, $n = 1, 2, 3, \ldots, 16$, $q = 1, 2, 3$. In the model $\mathbf{M}_2$, the RCSs of target 3 with respect to radar 7 and radar 8 are set as Fig.4, while the other RCSs are kept the same as $\mathbf{M}_1$.

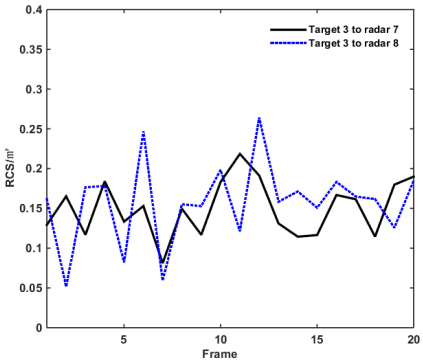

FIGURE 4. Time-varying reflectivity in RCS model $\mathbf{M}_2$.

A. SCENARIO 1: STEADY TARGET RCS

In this scenario, we only investigate the effect of the distance factor on resource allocation results. Thus, the RCS model $\mathbf{M}_1$ is adopted. To demonstrate the effectiveness of sensor scheduling, we shall make a comparison between our proposed scheduling method and the subset selection method developed in [33] (for a given tracking target, the radars with better path condition and better angular spread shall be chosen preferentially). In order to state conveniently, we define the following referential relationship: $\mathbf{e}_{\mathrm{opt}}$, $\mathbf{P}_{\mathrm{opt}}$, and β_{opt} correspond to the results of sensor scheduling, power allocation,

and bandwidth allocation calculated by our proposed method, respectively; $\mathbf{e}_{\text{bench}}$ represents the results of subset selection obtained by the method in [33]; $\mathbf{P}_{\text{uni}}$ and β_{uni} separately denote the uniformly allocated results of power and bandwidth resources.

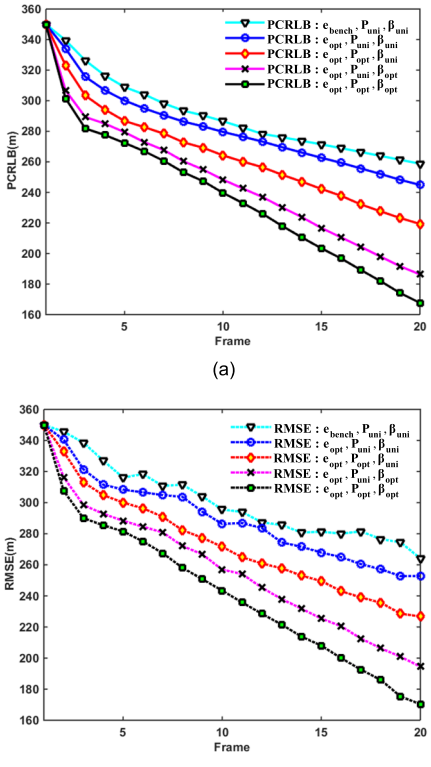

FIGURE 5. Performance comparison for the five methods in RCS model $\mathbf{M_1}$. (a) PCRLB performance. (b) RMSE performance.

Fig. 5 (a) and (b) show the tracking performance of the five methods from the perspectives of PCRLB and RMSE, respectively. In general, the sensor optimization scheduling integrated with power and bandwidth allocation performs best among all the methods. In addition, we note that the bandwidth optimization allocation performs better than the power optimization allocation. The interpretation can be found in (14) and (15), as the bandwidth has a quadratic form in the location submatrix of the PCRLB.

Fig.6 demonstrates the PCRLB comparison of each target under the proposed optimization method and the exhaustive search [34]. We all know that the exhaustive search is time-consuming but accurate, especially in the NP-hard problem. We can see from Fig. 6 that the close performance to the exhaustive search method is achieved by our proposed scheme. In addition, due to the path loss and angular spread, the tracking accuracy of target 2 is the worst, target 1 is the second, and target 3 is the best.

The details of sensor scheduling and power allocation results for each target in RCS model $\mathbf{M}_1$ are shown in Fig. 7, while the sensor scheduling and bandwidth allocation results

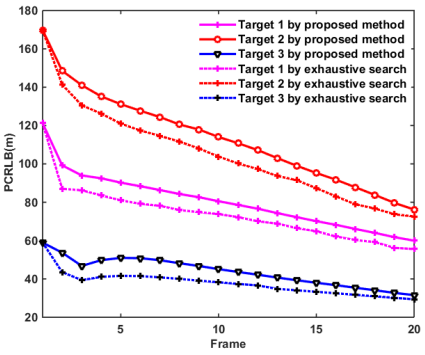

FIGURE 6. Comparison of each target's PCRLB by the proposed method and the exhaustive method [34] in RCS model $\mathbf{M_1}$.

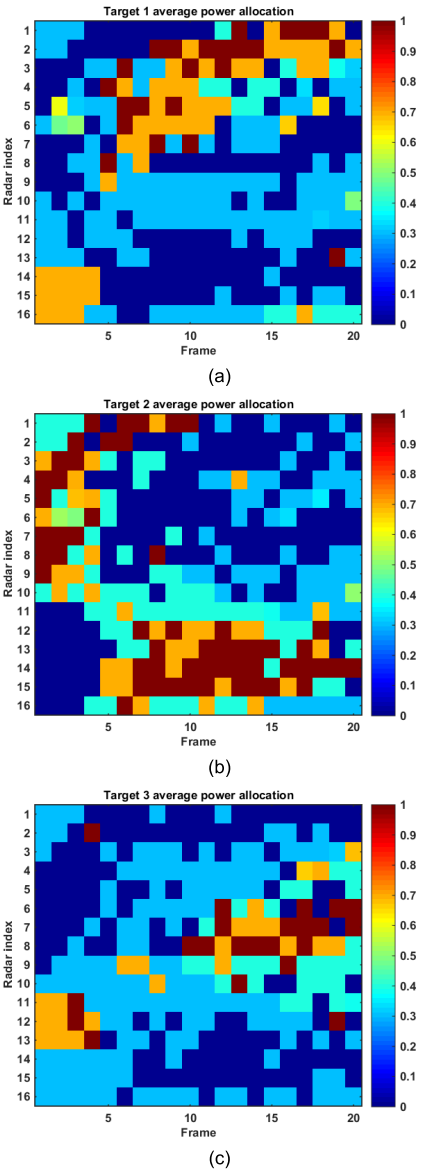

FIGURE 7. Sensor scheduling and power allocation results in the RCS model M1. (a) $q = 1$; (b) $q = 2$; (c) $q = 3$.

are represented in Fig. 8, where the grid colors denote the amount of allocated power and bandwidth for a radar node to track a certain target. Herein, the allocated power ratio and

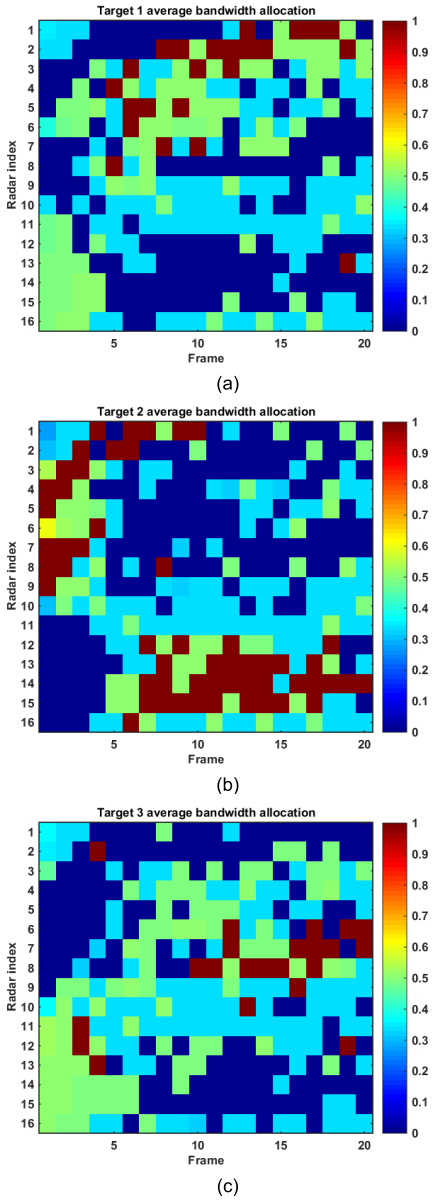

FIGURE 8. Sensor scheduling and bandwidth allocation results in RCS model $\mathbf{M}_1$. (a) $q = 1$; (b) $q = 2$; (c) $q = 3$.

bandwidth ratio are defined as:

$$\begin{cases} r_{n,q,k}^{power} = \dfrac{P_{n,q,k}}{P_{n,\text{total}}} \\ r_{n,q,k}^{bandwidth} = \dfrac{\beta_{n,q,k}}{\beta_{n,\text{total}}} \end{cases} \tag{35}$$

It can be seen that the target 2 consumes most of the system resources, which also can be proved in Fig. 6 where shows that target 2 is the worst tracking target. In addition, radar 14 and radar 15 are selected for target 2 frequently, which can be explain by that radar 14 and radar 15 are closest to target 2 and share better angular spread.

B. SCENARIO 2: FLUCTUANT TARGET RCS

To further reveal the effects of target RCS, the time-varying target RCS model $\mathbf{M}_2$ is adopted in this scenario. As such,

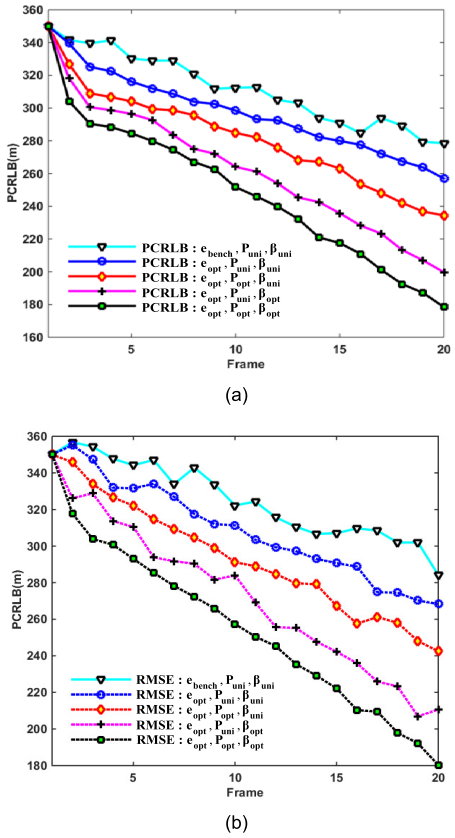

FIGURE 9. Performance comparison for the five methods in RCS model $\mathbf{M}_2$. (a) PCRLB performance. (b) RMSE performance.

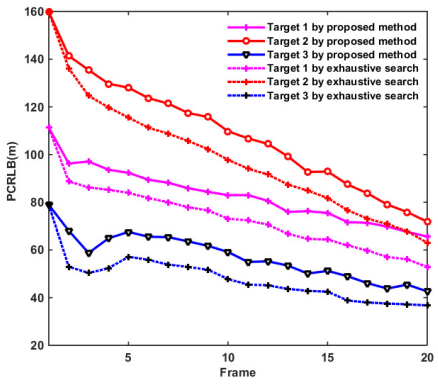

FIGURE 10. Comparison of each target's PCRLB by the proposed method and the exhaustive method [34] in RCS model $\mathbf{M}_2$.

the results of resource allocation are not only affected by the path loss and angular spread, but also influenced by the target RCS. The performance comparison for the five methods in the fluctuant target RCS model $\mathbf{M}_2$ is shown in Fig. 9.

It can be seen from Fig. 9 that the proposed method still has best performance among the five methods in the second RCS model $\mathbf{M}_2$. Since the target 3 has weaker reflectivity with respect to radar 7 and radar 8 in model $\mathbf{M}_2$ than in model $\mathbf{M}_1$, the tracking performances for all the methods have declined somewhat. In addition, it's worth noting that

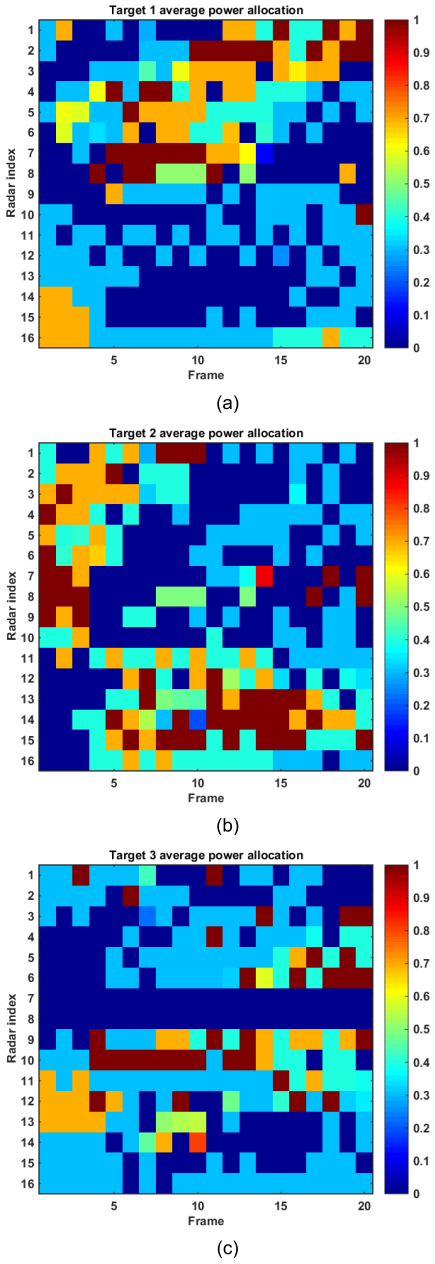

FIGURE 11. Sensor scheduling and power allocation results in RCS model $\mathbf{M}_2$. (a) $q = 1$; (b) $q = 2$; (c) $q = 3$.

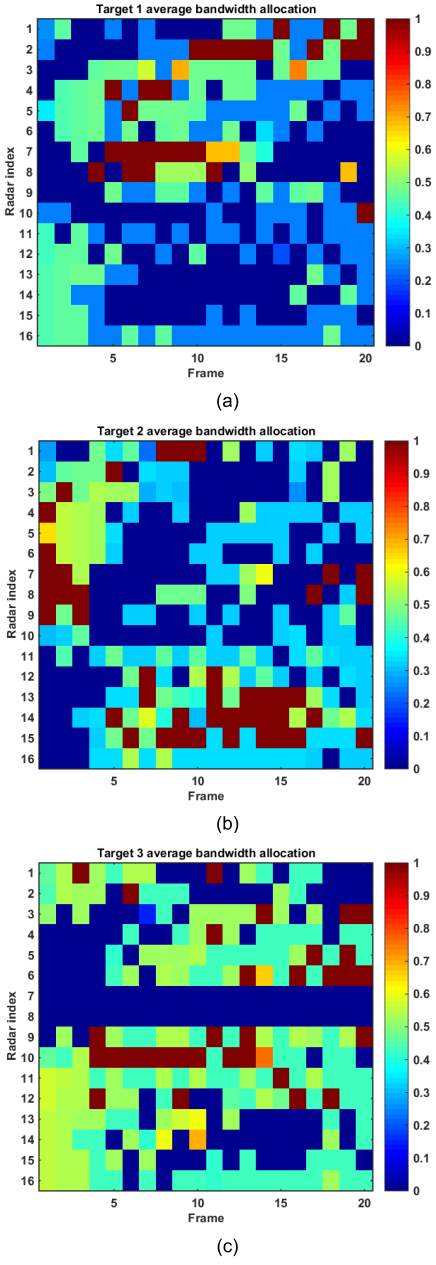

FIGURE 12. Sensor scheduling and bandwidth allocation results in RCS model $\mathbf{M}_2$. (a) $q = 1$; (b) $q = 2$; (c) $q = 3$.

when the target RCS fluctuates, the tracking performance also fluctuates accordingly.

The PCRLB comparisons of each target between the proposed optimization method and the exhaustive search [34] are given in Fig. 10. As the tracking performance of the proposed method is close to the exhaustive search algorithm, it can be seen that the proposed method can manage the limited resources of radar network system effectively. In addition, the tracking performance of target 3 decreases due to its weaker reflectivity to radar 7 and radar 8.

Fig. 11 and Fig. 12 show the resource allocation results in the second RCS model $\mathbf{M}_2$. Different from Fig. 7 and Fig. 8, radar 7 and radar 8 are not selected during the tracking of target 3, as target 3 has a weaker reflectivity with respect to radar 7 and radar 8. Thus, radar 7 and radar 8 are replaced by other radars (e.g. radar 9 and radar 10) with a path lose and better angular spread to track target 3. Consequently, in order to maintain the tracking performance of target 3, the resources of radar 7 and radar 8 are allocated to other radars.

In addition, to test the timeliness of the proposed method, its CPU time is compared with the exhaustive search's [34] in Fig. 13. Our simulation condition is MATLAB 2014a on a computer with 3.7GHz CPU and 8GB RAM. The results imply that compared with the exhaustive search [34], the proposed method possesses much lower computational complexity. It's crucial to note that the step length interval

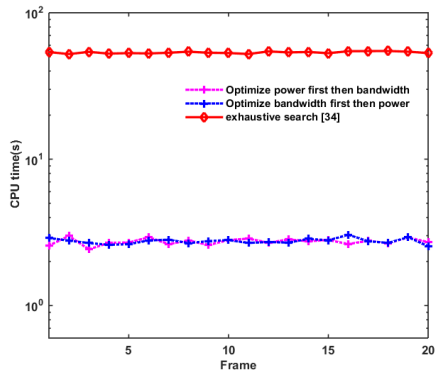

FIGURE 13. CPU time comparison.

of our simulation experiment is set as 5s, which implies that the proposed method can fully meet the real-time requirement. Besides, it is notable that the difference in the CPU time between the two methods (first optimize power then bandwidth and first optimize bandwidth then power) is less than 5%, which further proves the robustness of the proposed method and the optimization order of two variables can be swapped.

VI. CONCLUSION

In this paper, a sensor scheduling integrated with power and bandwidth allocation method is proposed for centralized MTT in the netted C-MIMO radar system. By introducing a set of convex relaxation technique and the cycle minimizer algorithm, the non-convex optimization problem is converted into a series of convex problems, which are solved by combining the SDP algorithm and the modified Frank-Wolfe feasible direction method. The effectiveness of the proposed method is demonstrated by numerical simulations.

ACKNOWLEDGMENT

The authors would like to thank the editors and the anonymous referees so much for their valuable time in helping us improve the presentation and quality of the manuscript.

REFERENCES

[1] H. Griffiths, "Multistatic, MIMO and networked radar: The future of radar sensors?" in *Proc. 7th Eur. Radar Conf.*, Paris, France, Sep./Oct. 2010, pp. 81–84.
[2] H. Zhang, W. Liu, Z. Zhang, W. Lu, and J. Xie, "Joint target assignment and power allocation in multiple distributed MIMO radar networks," *IEEE Syst. J.*, early access, May 13, 2020, doi: 10.1109/JSYST.2020.2986020.
[3] J. Yan, H. Liu, W. Pu, S. Zhou, Z. Liu, and Z. Bao, "Joint beam selection and power allocation for multiple target tracking in netted colocated MIMO radar system," *IEEE Trans. Signal Process.*, vol. 64, no. 24, pp. 6417–6427, Dec. 2016.
[4] Y. Lu, C. Han, Z. He, S. Liu, and Y. Wang, "Adaptive JSPA in distributed colocated MIMO radar network for multiple targets tracking," *IET Radar, Sonar Navigat.*, vol. 13, no. 3, pp. 410–419, Mar. 2019.
[5] M. Xie, W. Yi, T. Kirubarajan, and L. Kong, "Joint node selection and power allocation strategy for multitarget tracking in decentralized radar networks," *IEEE Trans. Signal Process.*, vol. 66, no. 3, pp. 729–743, Feb. 2018.
[6] H. Zhang, W. Liu, J. Xie, Z. Zhang, and W. Lu, "Joint subarray selection and power allocation for cognitive target tracking in large-scale MIMO radar networks," *IEEE Syst. J.*, vol. 14, no. 2, pp. 2569–2580, Jun. 2020.
[7] B. Ma, H. Chen, B. Sun, and H. Xiao, "A joint scheme of antenna selection and power allocation for localization in MIMO radar sensor networks," *IEEE Commun. Lett.*, vol. 18, no. 12, pp. 2225–2228, Dec. 2014.
[8] J. Li and P. Stoica, "MIMO radar with collocated antennas," *IEEE Signal Process. Mag.*, vol. 24, no. 5, pp. 106–114, Oct. 2007.
[9] J. Yan, B. Jiu, H. Liu, B. Chen, and Z. Bao, "Prior knowledge-based simultaneous multibeam power allocation algorithm for cognitive multiple targets tracking in clutter," *IEEE Trans. Signal Process.*, vol. 63, no. 2, pp. 512–527, Jan. 2015.
[10] J. Yan, H. Liu, B. Jiu, B. Chen, Z. Liu, and Z. Bao, "Simultaneous multibeam resource allocation scheme for multiple target tracking," *IEEE Trans. Signal Process.*, vol. 63, no. 12, pp. 3110–3122, Jun. 2015.
[11] H. Zhang, W. Liu, J. Xie, J. Shi, Z. Zhang, and W. Lu, "Space-time allocation for transmit beams in collocated MIMO radar," *Signal Process.*, vol. 164, pp. 151–162, Nov. 2019.
[12] Z. Li, J. Xie, and H. Zhang, "Joint power and time width allocation in collocated MIMO radar for multi-target tracking," *IET Radar, Sonar Navigat.*, vol. 14, no. 5, pp. 686–693, May 2020.
[13] H. Zhang, J. Xie, J. Shi, and Z. Zhang, "Antenna selection in MIMO radar with collocated antennas," *J. Syst. Eng. Electron.*, vol. 30, no. 6, pp. 1119–1131, 2019.
[14] W. Yi, Y. Yuan, R. Hoseinnezhad, and L. Kong, "Resource scheduling for distributed multi-target tracking in netted colocated MIMO radar systems," *IEEE Trans. Signal Process.*, vol. 68, pp. 1602–1617, 2020, doi: 10.1109/TSP.2020.2976587.
[15] N. Garcia, A. M. Haimovich, M. Coulon, and M. Lops, "Resource allocation in MIMO radar with multiple targets for non-coherent localization," *IEEE Trans. Signal Process.*, vol. 62, no. 10, pp. 2656–2666, May 2014.
[16] H. Zhang, J. Xie, J. Shi, Z. Zhang, and X. Fu, "Sensor scheduling and resource allocation in distributed MIMO radar for joint target tracking and detection," *IEEE Access*, vol. 7, pp. 62387–62400, Dec. 2019.
[17] J. Yan, W. Pu, S. Zhou, H. Liu, and Z. Bao, "Collaborative detection and power allocation framework for target tracking in multiple radar system," *Inf. Fusion*, vol. 55, pp. 173–183, Mar. 2020.
[18] H. Zhang, J. Xie, J. Shi, T. Fei, J. Ge, and Z. Zhang, "Joint beam and waveform selection for the MIMO radar target tracking," *Signal Process.*, vol. 156, pp. 31–40, Mar. 2019.
[19] S. Martello and P. Toth, *Knapsack Problems: Algorithms and Computer Implementations*. New York, NY, USA: Wiley, 1990.
[20] L. M. Kaplan, "Global node selection for localization in a distributed sensor network," *IEEE Trans. Aerosp. Electron. Syst.*, vol. 42, no. 1, pp. 113–135, Jan. 2006.
[21] S. Joshi and S. Boyd, "Sensor selection via convex optimization," *IEEE Trans. Signal Process.*, vol. 57, no. 2, pp. 451–462, Feb. 2009.
[22] H. L. Van Trees, *Detection, Estimation, and Modulation Theory, Part III: Radar–Sonar Signal Processing and Gaussian Signals in Noise*. New York, NY, USA: Wiley, 1971.
[23] H. L. Van Trees and K. L. Bell, *Bayesian Bounds for Parameter Estimation and Nonlinear Filter Tracking*. New York, NY, USA: Wiley, 2007.
[24] S. M. Kay, *Fundamentals of Statistical Processing, Volume I: Estimation Theory*. Hoboken, NJ, USA: Pearson, 1993.
[25] H. L. Van Trees, *Optimum Array Processing, Detection Estimation, and Modulation Theory—Part IV*. New York, NY, USA: Wiley, 2002.
[26] E. E. Tsakonas, N. D. Sidiropoulos, and A. Swami, "Optimal particle filters for tracking a time-varying harmonic or chirp signal," *IEEE Trans. Signal Process.*, vol. 56, no. 10, pp. 4598–4610, Oct. 2008.
[27] J. M. Pak, C. K. Ahn, Y. S. Shmaliy, and M. T. Lim, "Improving reliability of particle filter-based localization in wireless sensor networks via hybrid particle/FIR filtering," *IEEE Trans. Ind. Informat.*, vol. 11, no. 5, pp. 1089–1098, Oct. 2015.
[28] H. Zhang, J. Xie, J. Ge, W. Lu, and B. Liu, "Strong tracking SCKF based on adaptive CS model for maneuvering aircraft tracking," *IET Radar, Sonar Navigat.*, vol. 12, no. 7, pp. 742–749, Jul. 2018.
[29] H. Godrich, A. M. Haimovich, and R. S. Blum, "Target localization accuracy gain in MIMO radar-based systems," *IEEE Trans. Inf. Theory*, vol. 56, no. 6, pp. 2783–2803, Jun. 2010.
[30] P. Tichavsky, C. H. Muravchik, and A. Nehorai, "Posterior Cramer-Rao bounds for discrete-time nonlinear filtering," *IEEE Trans. Signal Process.*, vol. 46, no. 5, pp. 1386–1396, May 1998.
[31] C. Singh, P. Jirutitijaroen, and J. Mitra, "Monte Carlo simulation," in *Electric Power Grid Reliability Evaluation: Models and Methods*. Hoboken, NJ, USA: Wiley, 2019, pp. 165–183.
[32] W. W.-L. Li, Y. Shen, Y. J. Zhang, and M. Z. Win, "Robust power allocation for energy-efficient location-aware networks," *IEEE/ACM Trans. Netw.*, vol. 21, no. 6, pp. 1918–1930, Dec. 2013.

[33] H. Godrich, A. Petropulu, and H. V. Poor, "Cluster allocation schemes for target tracking in multiple radar architecture," in *Proc. Conf. Rec. 45th Asilomar Conf. Signals, Syst. Comput. (ASILOMAR)*, Pacific Grove, CA, USA, Nov. 2011, pp. 863–867.
[34] H. Kellerer, U. Pferschy, and D. Pisinger, *Knapsack Problems*. Berlin, Germany: Springer, 2004.

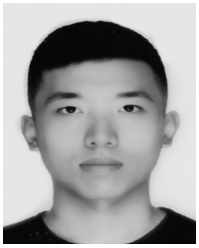

ZHENGJIE LI received the B.S. degree from the Air and Missile Defense College, Air Force Engineering University, Xi'an, Shaanxi, China, in 2018. He is currently pursuing the M.S. degree in weapon science and technology with Air Force Engineering University. His research interests include multifunction radar resource allocation, sensor scheduling, and multiple target tracking.

JUNWEI XIE received the bachelor's, master's, and Ph.D. degrees from Air Force Engineering University, Xi'an, Shaanxi, China, in 1993, 1996, and 2009, respectively. He is currently a Professor with Air Force Engineering University. He has published more than 100 refereed journal articles, book chapters, and conference papers. His research interests include novel radar systems and jamming and anti-jamming.

HAOWEI ZHANG received the bachelor's, master's, and Ph.D. degrees from the Air and Missile Defense College, Air Force Engineering University, Xi'an, Shaanxi, China, in 2014, 2016, and 2019, respectively. He is currently a Lecturer with Air Force Engineering University. His research interests include multifunction radar resource management and intelligent scheduling.

HOUHONG XIANG received the B.S. degree from the School of Information and Communication, Guilin University of Electronic Technology, in 2016. He is currently pursuing the Ph.D. degree with the National Laboratory of Radar Signal Processing, Xidian University. His research interests include signal processing, parameter estimation, and the applications of artificial neural networks on parameter estimation in radar systems.

ZHAOJIAN ZHANG received the bachelor's, master's, and Ph.D. degrees from the Air and Missile Defense College, Air Force Engineering University, Xi'an, Shaanxi, China, in 2011, 2013, and 2017, respectively. He is currently a Lecturer with the Air Force Early Warning Academy of PLA, Wuhan, Hubei, China. His research interests include novel radar systems and signal processing.